# Detection of Built-Up areas in Polarimetric SAR images

D. Borghys, C. Perneel and M. Acheroy

*Abstract*— **In this paper an approach to automatically detect built-up areas in high-resolution polarimetric SAR images is presented. First a set of features, mostly based on statistical properties of built-up areas in SAR images is defined. One feature is based on the isotropic spatial distribution of small uniform regions within agglomerations and avoids false alarms due to the presence of edges which the other features would introduce. The features are fused using logistic regression. Results of applying the method on an L-Band fully-polarised SAR image with a spatial resolution of about 1 m are shown.**

*Keywords*— **Detection of agglomerations, Built-up areas, Logistic Regression, Polarimetric SAR images**

## I. Introduction

In this paper an approach to automatically detect built-up areas in polarimetric SAR images is presented.

For a wide range of applications such as the study of the population density, the study of risks, planning of road networks, surveillance of the urban pressure on rural regions,... it is necessary to have an up-to-date overview of the location and the extent of the built-up areas. The fastest and cheapest way to obtain these updates is by extracting the information automatically from remote sensing data. Many papers describing the detection of built-up areas on visual or infrared satellite images (e.g. SPOT) have been published. At this moment, the most dramatic changes in the demographical situation occur in sub-tropical and tropical regions (mainly in Africa and Asia) where the climate (clouds) makes it difficult to use optical imagery for remote sensing applications. Detection of agglomerations is also important for registering images with maps, which is the first step in automatic cartography applications or change detection [1].

This paper will therefore focus on the detection of villages and built-up areas on SAR images as SAR can be acquired independent of the weather conditions. In particular a method is presented to detect built-up areas in high-resolution polarimetric SAR images. The method uses several statistical features obtained either directly from the images or after performing a region segmentation. These features are fused using logistic regression. The second section of this paper briefly discusses some statistical properties of SAR images. The third section presents the region segmentation method. Then the different features and the logistic regression are explained. In the last part the results obtained on a polarimetric (HH, HV and VV-polarisation) L-Band SAR image with a spatial resolution of 1 m are discussed.

Dirk Borghys is with the Signal & Image Centre of the Royal Military Academy, Renaissancelaan 30, B-1000 Brussels, Belgium, E-mail: Dirk.Borghys@elec.rma.ac.be

## II. Some Statistical properties of SAR images

Because of the properties of the speckle in SAR images, detectors (e.g. for linear features) that work well in visual or infrared images fail in SAR images. However, because for the major part of the images the statistics of the speckle can be modeled accurately, this information can be used in the development of a detector. The statistical distribution in uniform regions in the different types of images is well-known (see e.g. [2], [3] or any book about SAR). We will only use the single-look amplitude image (A) and the logarithm of the intensity ( $D = ln(A^2)$) for which the speckle in uniform regions follows a Rayleigh distribution and a Fisher-Tippett distribution respectively:

$$P(A) = \frac{A}{\sigma^2} exp\left(-\frac{A^2}{2\sigma^2}\right) \quad P(D) = \frac{exp(D)}{\sigma^2} exp\left(-\frac{exp(D)}{\sigma^2}\right) \tag{1}$$

The deterministic scatterers (diheders and triheders) found in villages [4] produce bright regions which cause the statistical distribution of the image value to differ highly from the theoretical distribution of uniform regions.

Another important aspect is the relationship between different components of multi-dimensional SAR images, i.e. the different polarisations. In vegetated areas the correlation between cross-polarised components (between HH/HV or VV/HV) is negligible [5]. In built-up areas, the presence of deterministic scatterers produces a much higher correlation between cross-polarised components. The amplitudes of the correlations between HH/HV and VV/HV approach the one found between HH/VV.

The features used in this article for the detection of agglomeration are based on these statistical properties.

## III. Image segmentation

The purpose of the image segmentation is to subdivide the image into uniform regions. In SAR images, the noise-like characteristics of the speckle cause classical segmentation methods to fail [2]. Especially methods based on measurements of local intensity are not well-suited for SAR. The only way to take into account the large point-to-point variations due to speckle is to consider the statistics of the image in the neighbourhood of the current pixel.

Such an approach is offered by the *Merge Using Moments* method [6]. MUM is a pure merge method, i.e. it starts from small areas of the image which are supposed to be homogeneous and then merges neighbouring areas if they comply with some similarity measure. In the original method [6] a Student-t test [7] is used to compare adjacent regions. In the case of multi-channel data this test can be replaced by its multi-variate version, the Hotellings $T^2$ test [7]. The method we used is based on the calculation of the Mahalanobis distance between the average vector of one region and the other region. The largest region is used to calculate the covariance matrix. If a uniform region is characterised by a multi-variate normal distribution, the square of the Mahalanobis distance of its elements follows a $\chi^2$-distribution with degree of freedom equal to the number of variables. The $\chi^2$-distribution could then be used to find a constant false alarm rate (CFAR) threshold (e.g. corresponding to an error of 5%).

However, when calculating the average of a region, the Mahalanobis distance of this average will be much smaller than that of the individual pixels in the region because we approach the average of the underlying distribution. Moreover, due to the spatial correlation in the SAR images, the elements of the covariance matrix will be underestimated. Furthermore, the quality of the estimate of both the covariance matrix and the mean vectors is influenced by the number of pixels that are used for the estimation. Both of these effects lead to an underestimation of the Mahalanobis distance.

The Mahalanobis distance will thus be a function of:

- The spatial correlation in the SAR image
- The number of pixels used to estimate the covariance matrix: $N_{ref}$
- The number of pixels used to calculate the average: $N_{mean}$

In order to find a CFAR threshold the effect of these parameters has to be modeled. To achieve that we simulated Fisher-Tippett distributed data (corresponding to log-intensity data in uniform regions [2]) with a spatial correlation function corresponding to the one found for the used SAR sensor. For a given combination of $N_{ref}$ and $N_{mean}$ a large number of samples was drawn and the histogram of the Mahalanobis distance calculated. From this histogram the 95, 99, 99.5 and 99.9 % thresholds were determined. Varying both $N_{ref}$ and $N_{mean}$ a 3D surface of thresholds is obtained (see fig 1).

This surface is used to adapt the threshold during the merge process, i.e. the threshold decreases as the size of the compared regions increases. The merge process is an iterative process. At each iteration the regions for which the ratio between the Mahalanobis distance and the found threshold is smallest are merged first. The result is that, for the same Mahalanobis distance, the smallest regions are merged first. The results of a segmentation based on this method using the 99.5% threshold is presented in fig 2. The unusual high threshold, only allowing 0.5 % of false alarms, causes an over-segmented image, but this is well-suited for the distance measure defined below.

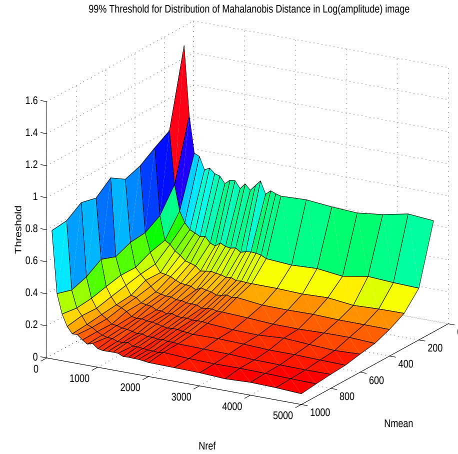


Fig. 1. Threshold for Mahalanobis distance vs. $N_{ref}$ and $N_{mean}$

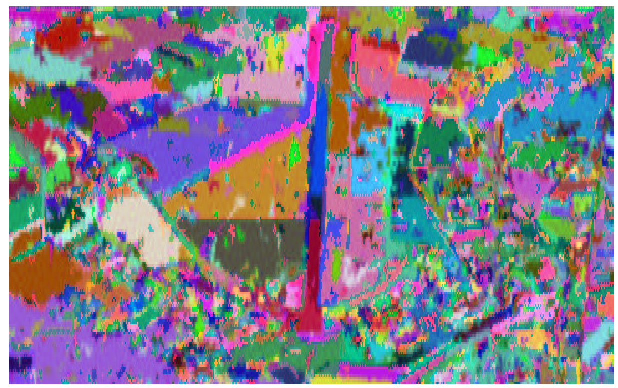

Fig. 2. Result of MUM

## IV. Description of the Features

### A. Introduction

The detection of built-up areas is based on the fact that the SAR image is not uniform in such areas. In many ways the statistics of built-up areas are different from those of uniform regions. This is the basis for the different features that are described below. Most features are calculated in small rectangular windows scanning the image. Only the first feature is calculated in the uniform regions found by the image segmentation discussed in the previous section.

### B. Distance measurement

This feature is based on the regions that were found by the image segmentation. The idea is that in a built-up area the uniform regions will be much smaller than in other parts of the image. However, this is also true for the edges between uniform regions. Hence the idea of linking a notion of isotropy to a measurement of region size. For each region its geometric centre is determined. From a geometric centre of one region, the closest centre to another region is determined along different directions. In practice the space around the current centre is divided in 8 parts (each corresponding to $45^o$) and in each part the smallest distance is kept. The "distance" feature is the next largest of these smallest distances. This is feature $F_1$. The smaller this distance, the more likely the region belongs to a built-up area. This procedure eliminates the problem of edges between uniform regions because for these types of regions the distance will be small only in a few directions.

### C. Skewness Measure

In uniform regions the amplitude image follows a Raleigh distribution which is skewed to the left. In built-up areas the distribution becomes more symmetric and can even be skewed to the right because of the presence of bright spots or bright lines. However, the classical definition of skewness can not be used as classical first order statistical estimators fail in SAR images, and particularly in regions containing deterministic reflectors, because they are to noisy and they are not sufficiently precise in agglomerations. The main reason is that a few isolated very bright spots have a very large influence on these estimators yielding results that are unstable.

We used an estimator of the skewness based on the median and two percentiles symmetrical around the median ( $P_t$ and $P_{1-t}$ with $0.0 \leq t < 0.50$ ) of the local grey-value distribution (cf. Yule):

$$F_2 = \frac{(P_{1-t} - P_{0.50}) - (P_{0.50} - P_t)}{P_{1-t} - P_t} \tag{2}$$

The estimator gives values bounded between -1 and +1. Negative values are obtained for distributions that are skewed to the left. To illustrate the problem with the classically defined skewness in agglomerations we calculated a skewness image for a small part of the SAR using the classical definition and the one based on percentiles ( with t=0.1 and a $20 \times 20$ window size). In fig 3 can be seen that isolated bright spots cause a patch pattern in the skewness value when the classical definition is used.

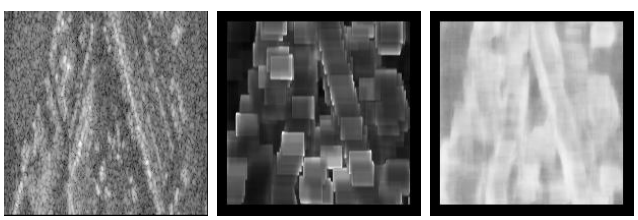

Fig. 3. Original image (left), classical skewness (centre), skewness based on percentiles (right)

### D. Variance Measure

For uniform regions the variance is solely due to the speckle. This variance is very low in the log-intensity image (and equal to a constant independent of the region [2]). In regions containing a lot of deterministic scatterers, the variance becomes much higher. We defined a measure of the variance, or rather of the lack of variance, analogously to the definition of the skewness:

$$F_3 = \frac{P_{0.75} - P_{0.25}}{P_{0.90} - P_{0.10}} \tag{3}$$

An advantage of this measure as opposed to the classically defined variance is the fact that it is bounded; in fact it is normalised between 0 and 1.

### E. Interchannel Correlation

In uniform regions with azimuthal symmetry (most vegetation) the correlation between cross-polarised components (i.e. between HH/HV and VV/HV) is very low. In areas with a lot of deterministic scatterers, such as diheders and triheders (e.g. in villages but also at the edges of forests) this correlation increases up to a level comparable to that of the correlation between co-polarised components (HH/VV). Therefore we also used these three interchannel correlations as features: $F_4 = C_{HH/HV}, F_5 = C_{VV/HV}, F_6 = C_{HH/VV}$.

### F. Overview of Feature Images

Calculating the different features in each pixel of the original image yields feature images. Fig. 4 shows the HH-polarised component of the original SAR image. The corresponding region of a map that was transformed into the coordinate space of the SAR image is shown in fig. 5. Fig. 6 to fig. 11 show the different feature images. The statistical parameters were calculated in a $40 \times 40$ window scanning the image except for the skewness that was calculated in a $20 \times 20$ window. All features were calculated using the log-intensity image except for the skewness which was calculated on the amplitude image. The figures show that the different features are complementary. Most of the features show the built-up areas either as bright or dark regions. False alarms consist mainly of edges between fields and forests. In the "distance image" the edges do not cause false alarms. We now need to find a way to combine the different features in order to obtain a good detection of agglomerations.

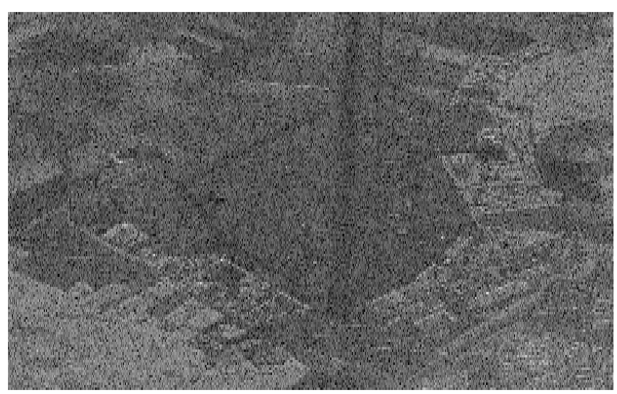

Fig. 4. Original image

Fig. 5. Part of map warped to image coordinates

Fig. 6. Image of Feature $F1$ (Distance Measure)

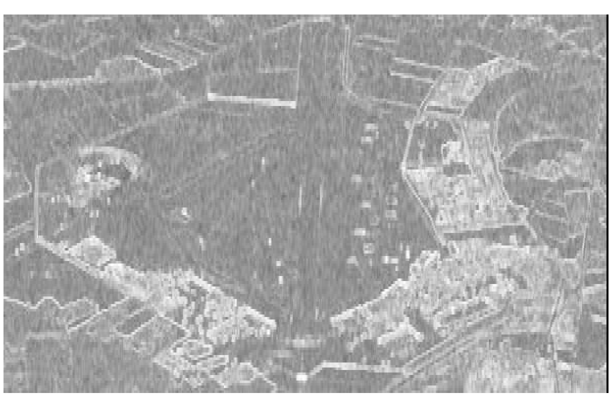

Fig. 7. Image of Feature $F_2$ (Skewness Measure)

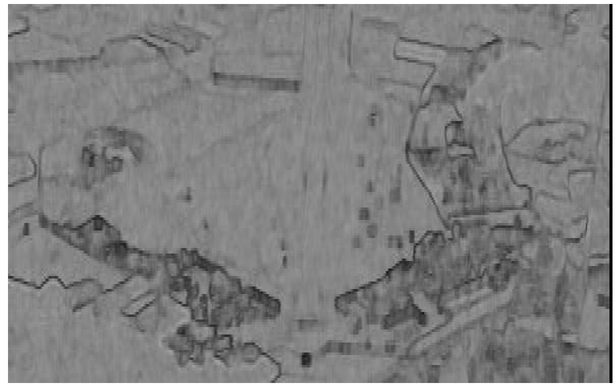

Fig. 8. Image of Feature $F_3$ (Variance Measure)

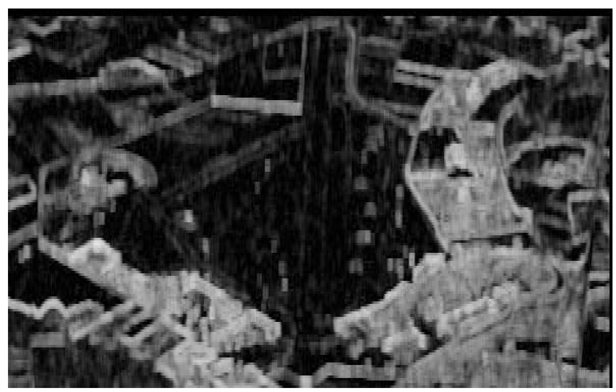

Fig. 9. Image of Feature $F_4(C_{HH/HV})$

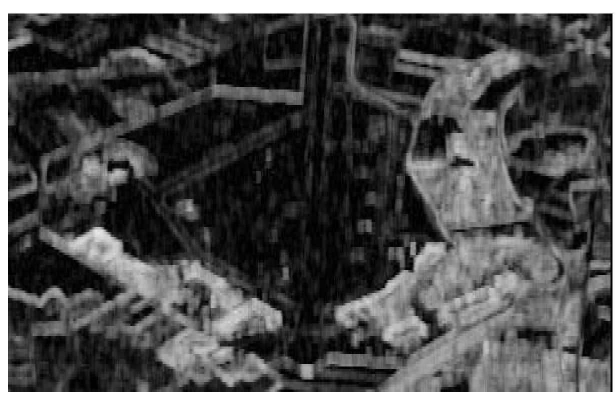

Fig. 10. Image of Feature $F_5(C_{VV/HV})$

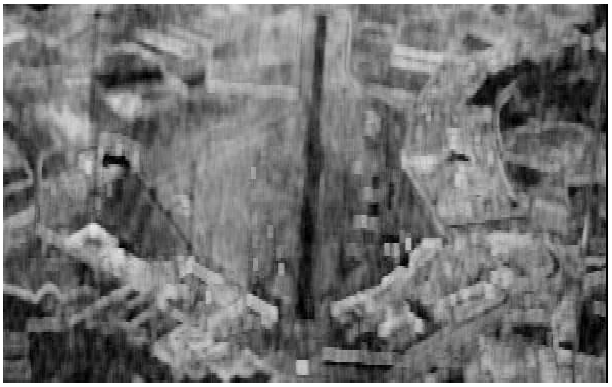

Fig. 11. Image of Feature $F_6(C_{HH/VV})$

## V. Feature Fusion using Logistic Regression

Logistic regression [8] offers a way to combine the different features while at the same time yielding a measure of their respective discriminative power. It is a supervised approach: In the $1200 \times 10000$ single-look image we identified a priori 1000 target (built-up areas) and 1000 background pixels to constitute the learning set. In the learning phase, at each pixel of the learning set, the different features were calculated and each set of features was labeled as belonging to the built-up area (1) or not (0).

Logistic regression is then used to find a combination of the form :

$$p_{xy}(target \mid \mathbf{F}) = \frac{e^{b_0 + \sum_i b_i F_i(x,y)}}{1 + e^{b_0 + \sum_i b_i F_i(x,y)}} \tag{4}$$

in which $p_{xy}(target \mid \mathbf{F})$ is the conditional probability that a pixel $(x, y)$ belongs to the class 1 given the vector of features $\mathbf{F}$ at the given pixel.

The logistic regression was carried out using Wald's forward method. In this method, at each step, the most discriminant feature is added and the significance of adding it to the model is verified. This means that not all feature will necessarily be included into the model. The Wald coefficient is a measure for the significance of the feature, i.e. its discriminative power for the given task. Table I shows the weights resulting from the logistic regression as well as the Wald coefficients.

TABLE I
Results of the Logistic Regression

| Name | Parameter Name | Weight | Wald |
|---|---|---|---|
| $F_1$ | Distance | -0.0401 | 159 |
| $F_2$ | Skewness | 0.0229 | 31.9 |
| $F_3$ | VarMeas | -0.0197 | 24.09 |
| $F_4$ | $C_{HH/HV}$ | 0.0140 | 6.24 |
| $F_5$ | $C_{VV/HV}$ | 0.0482 | 76.3 |
| $F_6$ | $C_{HH/VV}$ | -0.0326 | 53.4 |
| $F_0$ | Constant | 0.0112 | 0.0001 |

Apparently all features were selected. This supports the idea that they represent complementary information. The values of the Wald coefficient show that the most significant features are the distance and two of the correlations ( $C_{VV/HV}$ and $C_{HH/VV}$ ). The least significant (although still having non-zero weight) is the correlation $C_{HH/HV}$. This is not surprising as it is highly correlated with $C_{VV/HV}$.

## VI. Results and Discussion

Applying the weights found on the learning set to the complete feature image set gives the result shown in fig. 12. If a threshold of 90 % is applied on the output of the logistic regression most of the built-up areas are well detected. The effect of such a threshold is shown in fig. 13. In the figure the results are labelled using the ground truth extracted from the map. The dark regions are false alarms, the white ones are the correctly detected built-up areas, dark grey is the background and the light grey regions correspond to undetected parts of the built-up areas.

False alarms are found at the position of the motorway and especially at the cross-roads of the motorway. Some small false alarms do correspond to the edges between forests and fields. The false alarm at the top left is an earthen wall. The false alarms that remain are thus mainly due to regions in the image where deterministic scatterers are also likely to occur. If one is only interested in detecting large agglomerations most false alarms could be eliminated by constraining the size of the detected regions and eliminating narrow regions. Most of the so-called undetected parts are due to the crudeness of the ground truth, i.e. the contour of built-up areas was delimited but can still contain free spaces (fields, lawns,etc.).

In fig. 14 the probability of detection $P_d$ is plotted against the probability of false alarms $P_{FA}$. Points on this so-called ROC (receiver-operator curve) are obtained by varying the detection threshold. Please note that $P_{FA}$ and $P_d$ were both defined as ratios of surfaces, i.e. the false alarm probability is the ratio of the number of false alarm pixels to the total number of pixels in the image and the probability of detection was defined as the number of correctly detected pixels divided by the number of pixels contained in the built-up areas extracted from the map.

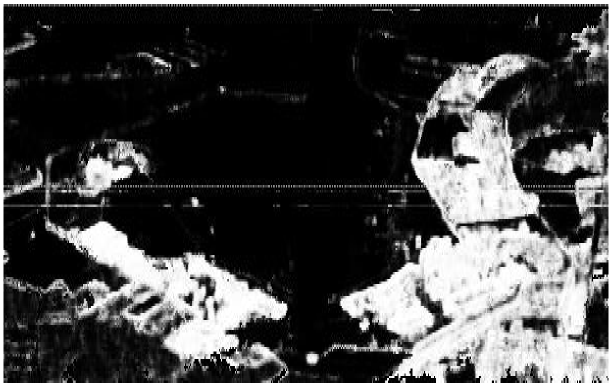

Fig. 12. Results of the logistic regression

Fig. 13. Ground truthed results at 90 % threshold. White=Correct Detection, Black=False Alarms, Light Grey=Undetected Areas

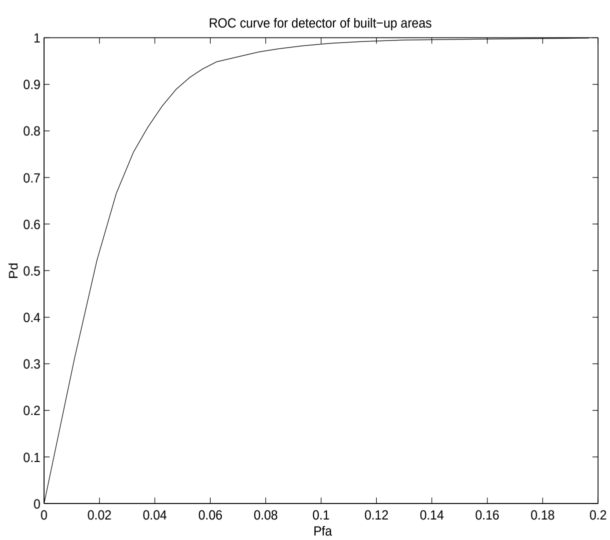


Fig. 14. ROC curve for the detector

## VII. Acknowledgments

The presented work is the result of a collaboration between the Signal & Image Centre of the Belgian Royal Military Academy and the Institut für Hochfrequenztechnik und RadarSysteme of the Deutshes Zentrum für Luft- and Raumfahrt (DLR), who also provided the images. The images used in this project are acquired by DLR's E-SAR system.

## VIII. Conclusions

A new method for detecting built-up areas using full-polarimetric SAR images was presented. The method is based on a combination of some simple statistical estimators. The estimators were designed to cope with the large dynamics of the SAR amplitudes in agglomerations. Logistic regression has shown that the polarimetric features (the interchannel correlations) are among the most discriminating features of those that were used. The logistic regression yields an image on which all built-up regions have been well selected and with false alarms only due to other types of extended vertical structures. False alarms due to edges between fields and forests were avoided by introducing a feature (distance measurement) based on the isotropy of the spatial distribution of small uniform regions within built-up areas.

## References

[1] M. Roux, *Recalage d'images multi-sources, application au recalage d'une image SPOT et une carte.* PhD thesis, ENST, Paris, September 1992.

[2] C. Oliver and S. Quegan, *Understanding Synthetic Aperture Radar Images.* Boston-London: Artech House, 1998.

[3] J. Curlander and R. McDonough, *Synthetic Aperture Radar: Systems and Signal Processing.* New York: John Wiley & Sons, 1991.

[4] C. Gouinaud, *Traitement d'images satellitaires pour la détection d'agglomérations.* PhD thesis, ENST, Paris, December 1996.

[5] E. Rignot, R. Chellappa, and P. Dubois, "Unsupervised segmentation of polarimetric sar data using the covariance matrix," *IEEE Geoscience and Remote Sensing*, vol. 30, no. 4, pp. 697–704, 1992.

[6] R. Cook, I. M. Connell, and C. Oliver, "Mum (merge using moments) segmentation for sar images," in *Proc. of the 1994 Data Processing for Remote Sensing*, no. Vol. 2316, SPIE, SPIE, April 1994.

[7] T. Anderson, *Introduction to Multivariate Statistical Analysis.* New York: John Wiley & Sons, 1958.

[8] D. Hosmer and S. Lemeshow, *Applied Logistic Regression.* John Wiley and Sons, 1989.